JOURNAL OF GEOPHYSICAL RESEARCH, VOL. 103, NO. D18, PAGES 23,163-23,172, SEPTEMBER 27, 1998

Can interannual land surface signal be discerned in composite AVHRR data?

J. Cihlar, J.M. Chen and Z. Li
Applications Division, Canada Centre for Remote Sensing, Ottawa

F. Huang and R. Latifovic
Intermap Information Technologies (Canada) Ltd., Ottawa

R. Dixon
Manitoba Remote Sensing Centre, Winnipeg

Abstract. The ability to make repeated measurements of the changing Earth's surface is the principal advantage of satellite remote sensing. To realize its potential, it is necessary that true surface changes be isolated in the satellite signal from other effects which also influence the signal. In this study, we explore the magnitude of such effects in composite NOAA advanced very high resolution radiometer (AVHRR) images with a pixel spacing of 1 km. A compositing procedure is frequently used in the preparation of data sets for land biosphere studies to minimize the effect of clouds. However, the composite images contain residual artifacts which make it difficult to compare measurements at various times. We have employed a 4-year (1993-1996) AVHRR data set from NOAA 11 and 14 covering the Canadian landmass and corrected these data for the influence of the remaining clouds (full pixel or subpixel), atmospheric attenuation, and bidirectional reflectance. We have found that such corrections are essential for studies of interannual variations. The magnitude of the interannual signal varied with the AVHRR channel, land cover type, and satellite sensor but it was reduced by a factor of 2 to 8 between top of the atmosphere and the normalized surface reflectance. The remaining variations consisted of true interannual signal and the residual noise in the data (including sensor calibration) which was not removed by the correction process. Assuming that barren or sparsely vegetated land in northern Canada has not changed over the 4-year period, the mean residual uncertainty in surface reflectance of the selected sites was 0.012 for AVHRR channel 1, 0.042 for channel 2, and 0.068 for the normalized difference vegetation index (NDVI). These values decreased to 0.011, 0.024 and 0.038, respectively, when excluding 1994 data because their atmospheric and bidirectional corrections were hampered by high solar zenith angles (mean values above 55° in all 1994 composite periods). The errors could be further reduced by more refined corrections for bidirectional and atmospheric effects. The impact of the uncertainty of channel 1 and 2 measurements is also significantly diminished by using ratio indices such as the NDVI. It is concluded that interannual variability exceeding 0.015-0.038 in NDVI (averaged over multiple pixels) can be detected for similar data sets and conditions, provided that sensor calibration does not introduce additional errors. Since such errors can be large for some conditions and applications, the importance of accurate sensor calibration cannot be overemphasized.

1. Introduction

A fundamental strength of satellite Earth observations is the capability to monitor the dynamics of the Earth's surface and to quantify the changes that take place, thus providing a basis for understanding the temporal trends and their significance. In using satellite sensors as measuring instruments it is critically important that the measured and inferred quantities be an accurate representation of the Earth's environment at the time of imaging. This problem can be understood in two steps, the representation of the reflectance or emission characteristics of the surface, and the inversion of these measurements in terms of the physical or other surface state variables. The first step thus deals with measurement issues which include sensor calibration, atmospheric corrections, and geometric effects on the measured signal and its relation to the radiation reflected or emitted by the target of interest. The second step involves the study of landscape dynamics.

The measurement issues are particularly relevant in the case of the advanced very high resolution radiometer (AVHRR), a sensor originally not designed for terrestrial monitoring but nevertheless used extensively for this purpose [*Townshend*, 1994; *Los et al.*, 1994; *Sellers et al.*, 1994; *Myneni et al.*, 1997]. Because of the daily imaging of the entire globe, this sensor provides sufficient data to reconstruct the spatiotemporal dynamics of the interaction between the

Paper number 98JD00050.
0148-0227/98/98JD-00050$09.00

atmosphere and the terrestrial biosphere, principally by observing changes related to green leaf area. The modest spatial resolution (1.1 km at nadir) leads to a manageable data volume, thus making it feasible to process daily data over large areas. However, AVHRR does not have onboard calibration and the target - sensor geometry varies greatly on various time scales, from days to years, due to the wide imaging swath and the orbit precession. In addition, accurate atmospheric correction is difficult because the state of the atmosphere (especially aerosols and water vapor) is not well determined at the time of imaging. It is therefore likely that when AVHRR data are used to monitor seasonal and interannual trends, some of the detected changes are in fact residual artifacts rather than true changes in the target. Since these changes are often directional (e.g., changes in orbit), temporal averaging does not provide a satisfactory solution.

Substantial efforts have been devoted to developing accurate methods for dealing with the possible sources of radiometric noise in the AVHRR data. Various sensor calibration techniques have been developed over the years [*Teillet and Holben*, 1994; *Rao and Chen*, 1994; *Rao et al.*, 1994; *Vermote and Kaufman*, 1995; *Los et al.*, 1994]. These methods work best when applied to retrospective data. However, many AVHRR data sets are produced in quasi-real time, thus necessitating the projection of any changes in calibration trends into the future [*Cihlar and Teillet*, 1995]. Also, diverse atmospheric correction techniques have been applied [*Teillet*, 1992; *Rahman and Dedieu*, 1994; *Eidenshink and Faundeen*, 1994; *James and Kalluri*, 1994]. Various methods have been applied to the identification and removal of geometric and other remaining effects from the data, ranging from empirically derived partial corrections [*Los et al.*, 1994; *Sellers et al.*, 1994; *Gutman*, 1991, 1994; *Cihlar and Howarth*, 1994] to more comprehensive approaches [*Gutman et al.*, 1995; Cihlar et al., 1997a]. In the latter case, the recent ABC3 methodology (atmospheric, bidirectional and contamination corrections of the Canada Centre for Remote Sensing [*Cihlar et al.*, 1997a]) includes bidirectional corrections of channels 1 and 2, identification and removal of pixels contaminated by differential atmospheric effects (subpixel clouds, fog, smoke) or snow, and atmospheric and surface emissivity corrections for AVHRR channel 4.

In this paper we have attempted to address the question, How accurately can the surface signal be detected in a multiyear series of AVHRR measurements? Although AVHRR data are used here, the considerations apply to similar sensors, such as MODIS (moderate resolution imaging spectrometer [*Salomonson*, 1988]), MERIS (medium resolution imaging spectrometer [*European Space Agency*, 1995]) and VEGETATION [*Saint*, 1992]. In all these cases the raw data contain much noise, in addition to the land surface signal. The noise is related to sensor calibration; cloud cover which typically obscures >50% of the image; fog, smoke, or residual (subpixel) clouds; clear sky atmospheric attenuation (water vapor, etc.); bidirectional reflectance effects, especially due to the wide field of view of these sensors; and other factors.

2. Theory

In using AVHRR data for terrestrial surface studies, the raw images over a period of time are typically coregistered and subsequently combined to form nearly cloud-free composites. Since adjacent pixels originate at different times and imaging conditions as well as geometry, the composites are more difficult to analyze quantitatively. In a composite AVHRR image, the retrieved surface reflectance ρ_{RETR} for a pixel i,j and time period t given a standardized viewing geometry (e.g., nadir viewing and solar zenith angle of 45° [*Cihlar et al.*, 1997a, b] can thus be regarded as consisting of several components:

$$\rho_{RETR}(i,j,t) = \rho_{TRUE}(i,j,t)(1\pm\varepsilon_{CAL}(i,j,t))(1\pm \varepsilon_{ATM}(i,j,t))(1\pm\varepsilon_{BRDF}(i,j,t)) \pm\varepsilon_{REG}(i,j,t), \quad (1)$$

where

ρ_{TRUE} the true surface reflectance at the standardized viewing geometry (dimensionless);

ε_{CAL} measurement error due to incorrect sensor calibration (dimensionless);

ε_{ATMO} error due to atmospheric effects (dimensionless);

ε_{BRDF} error due to bidirectional effects (dimensionless);

ε_{REG} error due to the misregistration of individual pixels used in the composite (dimensionless).

Among these, the registration error $\varepsilon_{REG}(i,j,t)$ is essentially random and thus approaches zero when averaging over similar pixels (i,j,t), composites t, or both. The magnitude of the bidirectional error $\varepsilon_{BRDF}(i,j,t)$ depends on cover type, and it may also depend on the time within the growing season as well as the year (when the correction coefficients are derived separately every year). The ability to remove the atmospheric error $\varepsilon_{ATMO}(i,j,t)$ depends on the knowledge of the atmospheric constituents and the quality of the atmospheric model. When fixed climatological values are used, $\varepsilon_{ATMO}(i,j,t)$ is likely to vary systematically with location/latitude and season because the key parameters (water vapor, aerosols) also vary in this fashion. The deficiencies of the atmospheric model will have a systematic effect (inadequate parameterization of the radiation processes in the atmosphere) and a random effect (e.g., due to extreme geometry of the pixels retained in the composite) on the corrected signal. In addition, there will be a random error due to the inadequate knowledge of the atmospheric state at the time of imaging. Finally, the calibration error $\varepsilon_{CAL}(i,j,t)$ will vary only with time t; such variability can be quantified [e.g., *Rao et al.*, 1994] although residual errors in this quantification cannot be ruled out.

Assuming that the errors for a given pixel are independent of each other, equation (1) can also be written as

$$\rho_{RETR}(i,j,t) = \rho_{TRUE}(i,j,t) \pm \Delta\rho_{CAL}(i,j,t) \pm \Delta\rho_{ATMO}(i,j,t) \pm \Delta\rho_{BRDF}(i,j,t) \pm \Delta\rho_{REG}(i,j,t), \quad (2)$$

where:

$$\Delta\rho_{CAL}(i,j,t) = \rho_{TRUE}(i,j,t)\varepsilon_{CAL}(i,j,t), \quad (3a)$$

$$\Delta\rho_{ATMO}(i,j,t) = \rho_{TRUE}(i,j,t)(1\pm\varepsilon_{CAL}(i,j,t))\varepsilon_{ATMO}, \quad (3b)$$

$$\Delta\rho_{BRDF}(i,j,t) = \rho_{TRUE}(i,j,t)(1\pm\varepsilon_{CAL}(i,j,t))(1\pm\varepsilon_{ATMO}(i,j,t))\varepsilon_{BRDF} \quad (3c)$$

$\Delta\rho_{CAL}$, $\Delta\rho_{ATMO}$, and $\Delta\rho_{BRDF}$ thus represent errors in the retrieved surface reflectance of pixel (i,j,t) obtained as a result of imperfect corrections.

When averaged over a number of pixels (i,j,t) and the period dt during the growing season, the mean surface reflectance for these pixels $\rho(dt)$ will be:

$$\rho_{RSTR}(dt) = \rho_{TRUE}(dt) \pm \Delta\rho_{CAL}(dt) \pm \Delta\rho_{ATMO}(dt) \pm \Delta\rho_{BRDF}(dt). \quad (4)$$

The difference between surface reflectance retrieved in two different years $d\rho$ will then be

$$d\rho_{RSTR} = \rho_{RSTR}(dt_2) - \rho_{RSTR}(dt_1) = d\rho_{TRUE} \pm d\rho_{CAL} \pm d\rho_{ATMO} \pm d\rho_{BRDF}. \quad (5)$$

The interannual reflectance difference thus consists of potential residual errors in sensor calibration, atmospheric correction, and bidirectional correction, in addition to changes in the target itself. As noted above, all these can have a systematic component, although its magnitude will depend on several factors and the overall impact is thus not in general predictable.

If the surface reflectance has not changed between t_1 and t_2 and all corrections were made accurately, $d\rho$=0. For time invariant targets, the magnitude of the $d\rho$ at a given processing stage is therefore a measure of the residual errors remaining in the data.

3. Data and Methods

We employed AVHRR data of Canada processed by the Geocoding and Compositing System (GEOCOMP [*Robertson et al.*, 1992]) and subsequently corrected using the algorithms embedded in the ABC3 methodology [*Cihlar et al.*, 1997a]. NOAA 11 (1993, 1994) and NOAA 14 (1995, 1996) AVHRR data were used. Although the time series is fairly short, it includes two important effects: change of the AVHRR sensor, and an extreme data acquisition geometry with large solar zenith angles during 1994. Briefly, the GEOCOMP processing yields a set of composite images every 10 days during the growing season for the Canadian landmass consisting of the five AVHRR channels (in radiance or apparent temperature units) and the three angles describing the acquisition geometry of each pixel (solar and view zenith, and relative azimuth); the maximum NDVI is used to select the composite pixel among all the candidates acquired during the compositing period [*Cihlar et al.*, 1997a]. The radiometric sensor calibration is based on the piecewise linear model [*Teillet*, 1992; *Cihlar and Teillet*, 1995] for channels 1 and 2 which accounts for postlaunch sensor degradation. The ABC3 processing incorporates atmospheric corrections based on the SMAC model (simplified method for atmospheric corrections [*Rahman and Dedieu*, 1994]. The SMAC processing was carried out assuming water vapor content of 2.3 g/cm^2, ozone content of 0.319 cm atm, and optical depth of 0.05 at 550 nm found by *Ahern et al.* [1991] for summer conditions in eastern Canada. Pixels contaminated by clouds, smoke, etc., are identified using the CECANT algorithm (cloud elimination from composites using albedo and NDVI trend [*Cihlar*, 1996]). CECANT is based on high NDVI sensitivity to the presence of clouds, aerosols, or snow. It uses (1) the high contrast between the albedo (represented by AVHRR channel 1) of land, especially when fully covered by green vegetation as opposed to clouds or snow/ice and (2) the monotonic NDVI trend (increase to peak green, decrease thereafter). Threshold values are established on the basis of the statistics in each compositing period. ABC3 bidirectional reflectance corrections were made using a modified Roujean model [*Roujean et al.*, 1992; *Wu et al.*, 1995; *Li et al.*, 1996], by deriving land cover-specific coefficients for the generic model and incorporating a hotspot correction [*Chen and Cihlar*, 1997]; land cover of Canada [*Pokrant*, 1991] was used for this purpose. After these corrections, pixels identified as being contaminated were replaced by temporal interpolation. The details on the ABC3 procedure and the above processing steps are given by *Cihlar et al.* [1997a]. It should be noted that the identification of contaminated pixels and BRDF corrections were based on coefficients derived separately for each year, except for 1994 for which the 1993 coefficients were used to partly compensate for the extreme sensing geometry. The result of this processing is surface reflectance in AVHRR channels 1 (C1) and 2 (C2) corrected to a standard viewing geometry (nadir view, solar zenith angle 45°) and the normalized difference vegetation index (NDVI) computed from C1 and C2, at 10-day intervals for Canada during the growing season. To reduce the data volume for analysis in this study, the data set was subsampled and only every sixth line and sixth pixel (pixel size 1 km) was retained.

Using a land cover map [*Pokrant*, 1991], several sites with various dominant cover types were selected (Table 1). It should be noted that these sites may contain other cover types, although the indicated cover is dominant in each area. In these areas the means for each channel were computed for the period June 1 to August 31 of each year. The calculation included only land pixels and was repeated with data at four processing stages: TOA (top of the atmosphere) which included only sensor calibration and conversion from radiance to reflectance; after atmospheric corrections, thus representing the apparent surface reflectance (ATMO); after bidirectional corrections which accounted for differences in imaging geometry (BRDF); and after interpolation where the contaminated pixels were replaced by temporal interpolation (NORM). For TOA and NORM, means were computed for all land pixels, but in case of ATMO and BRDF only uncontaminated (as determined by CECANT) land pixels were included in computing the mean value.

4. Results and Discussion

4.1. Effectiveness of Data Corrections

The data set entails four primary variables: AVHRR channel, site (Table 1), year of AVHRR data acquisition, and the stage of corrections. In general, spectral reflectance ρ decreased as more corrections were made, while NDVI increased. The removal of contaminated pixels (TOA_ALL→TOA) caused a large change, especially for channel 1 and in northern areas. In the case of the NDVI, generally a small increase was found, as would be expected from the removal of cloud/aerosol-or snow contaminated pixels.

For channel 1 (Figure 1), the decrease in ρ from TOA to ATMO was primarily due to corrections for Rayleigh scattering. The between-years range of mean values also decreased somewhat between the two processing stages.

Table 1. Description of sample locations

Site	Upper Left Corner Line, Pixel, (Dimensions; Number of Pixels*)	Cover	Location
1 RAN-SA	244,594, (15x15; 225)	grassland	southern Alberta
2 CON-SLA	297,460, (20x20; 400)	coniferous forest	south of Lake Athabasca
3 MIX-ELS	570,665, (20x20; 400)	mixed wood forest	east of Lake Superior
4 TUN-EHB	630,450, (20x20; 400)	tundra	east of Hudson Bay
5 BL-QM	385,335, (20x20; 400)	barren land	south of Queen Maud Gulf
6 BL-MEI	300,210, (80x80;6400)	barren land	Melville Island
7 BL-DK	450,590, (80x80;6400)	barren land	District of Keewatin
8 BL-UNP	585,385, (60x60;3600)	barren land	Ungava Peninsula

*Water pixels excluded from the analysis

While the TOA→ATMO reduction varied somewhat depending on cover type and year, the reduction due to BRDF variations (ATMO→BRDF) was significant. Generally, the BRDF correction further reduced the interannual range, but this did not occur consistently. For example, the BRDF corrections for grassland (Figure 1a) and coniferous forest (Figure 1b) appear to be somewhat high for 1994, in spite of using coefficients from 1993. In 1994, many solar zenith angle (SZA) values were >55° (Figure 2) but the normalization was done to SZA=45°. According to *Rahman and Dedieu* [1994] the SMAC model is less accurate when SZA>60°. The lack of strong convergence after BRDF

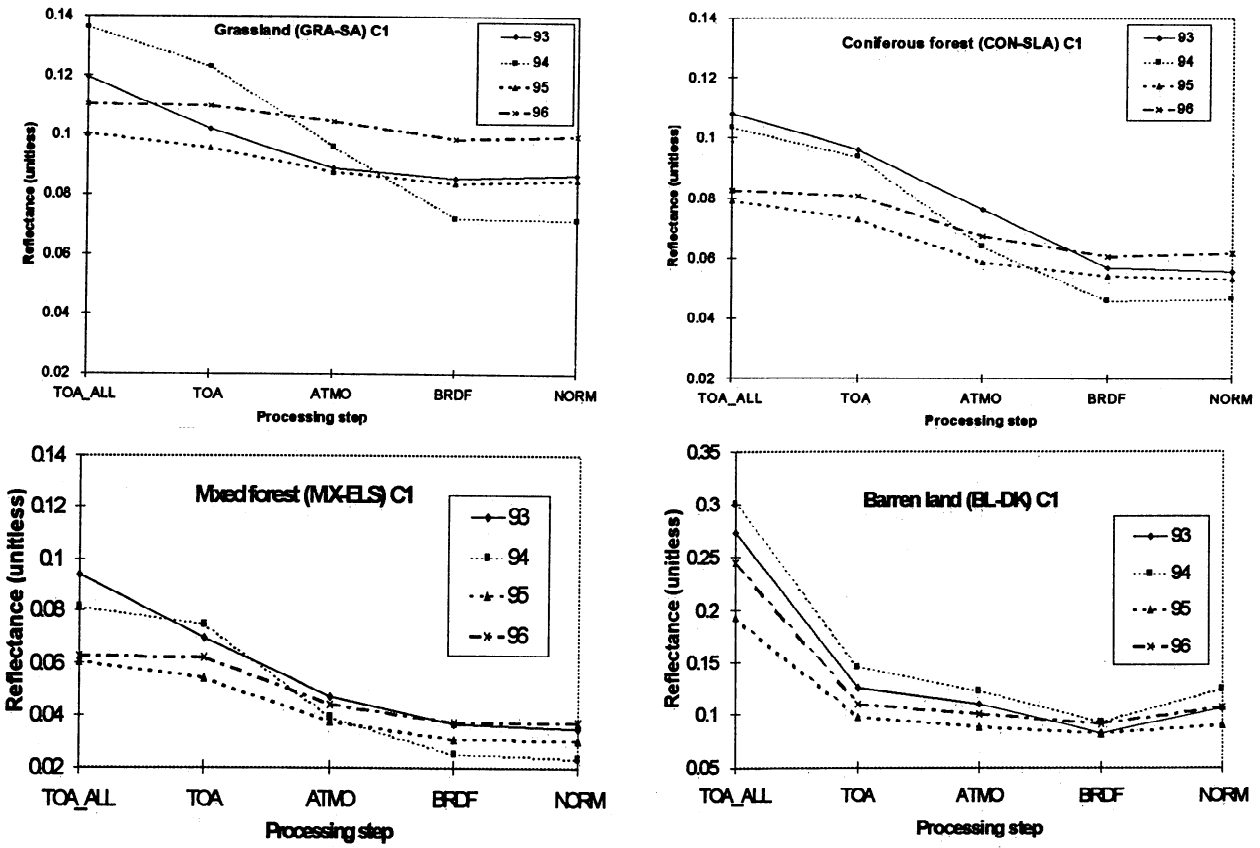

Figure 1. Mean AVHRR channel 1 reflectance for various sites, degree of corrections, and years. TOA, ATMO, BRDF, and NORM refer respectively to data corrected for sensor effects, atmospheric effects, bidirectional effects, and eliminated pixels. The land cover types represented are (a) grassland, (b) coniferous forest, (c) mixed forest, and (d) barren land.

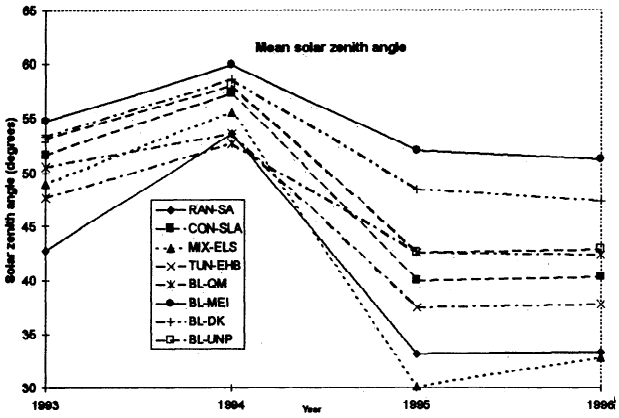

Figure 2. Mean solar zenith angle values for various sites and years.

corrections could thus be the combined effect of imperfect atmospheric and bidirectional corrections. The effect was even more pronounced when BRDF coefficients were derived from the 1994 data in a trial procedure. - The difference between BRDF and NORM was small, as expected. This is because the contaminated pixels (eliminated before TOA) are replaced in NORM by temporal interpolation. The interpolation was less successful for northern sites where only few non-contaminated pixels were present (Figure 1d), often as low as three during the entire growing season.

The range of mean C1 values among years was highest at the TOA level and decreased at the higher processing stages. The reduction was largest for barren land (Figure 1d and others not shown). The differences were also substantive for forest cover types (Figures 1b and 1c). Since the 1994 data were most often responsible for the lack of convergence among years, it is likely that the large SZA values (Figure 2) were at least partly responsible for the observed trend. Given that the barren areas occur in the north and have large SZAs every year, the relative effect of the extreme geometry in 1994 would be smaller.

In AVHRR channel 2, the atmospheric corrections (TOA→ATMO) did not decrease the interannual range (Figure 3). This is principally because the main atmospheric effect is due to the column water vapor, and this correction was made simplistically during the processing since only a constant column value was assumed for all the processed data. Given that the atmospheric water vapor content varies greatly in the spatial as well as temporal dimensions and since actual measurements (e.g., radiosondes) are very sparse, the C2 atmospheric corrections could not account for it in detail. In most cases, the range of values increased between TOA and ATMO. The increase is attributed to the value of the total column water used (2.3 g/cm^2), commonly used for mid-latitude summer conditions. A subsequent check of reanalyzed data (Kalnay et al., 1996) suggested that over Canada, summer values range mostly between 0.8 and 1.6 g/cm^2. A high column water value would artificially increase

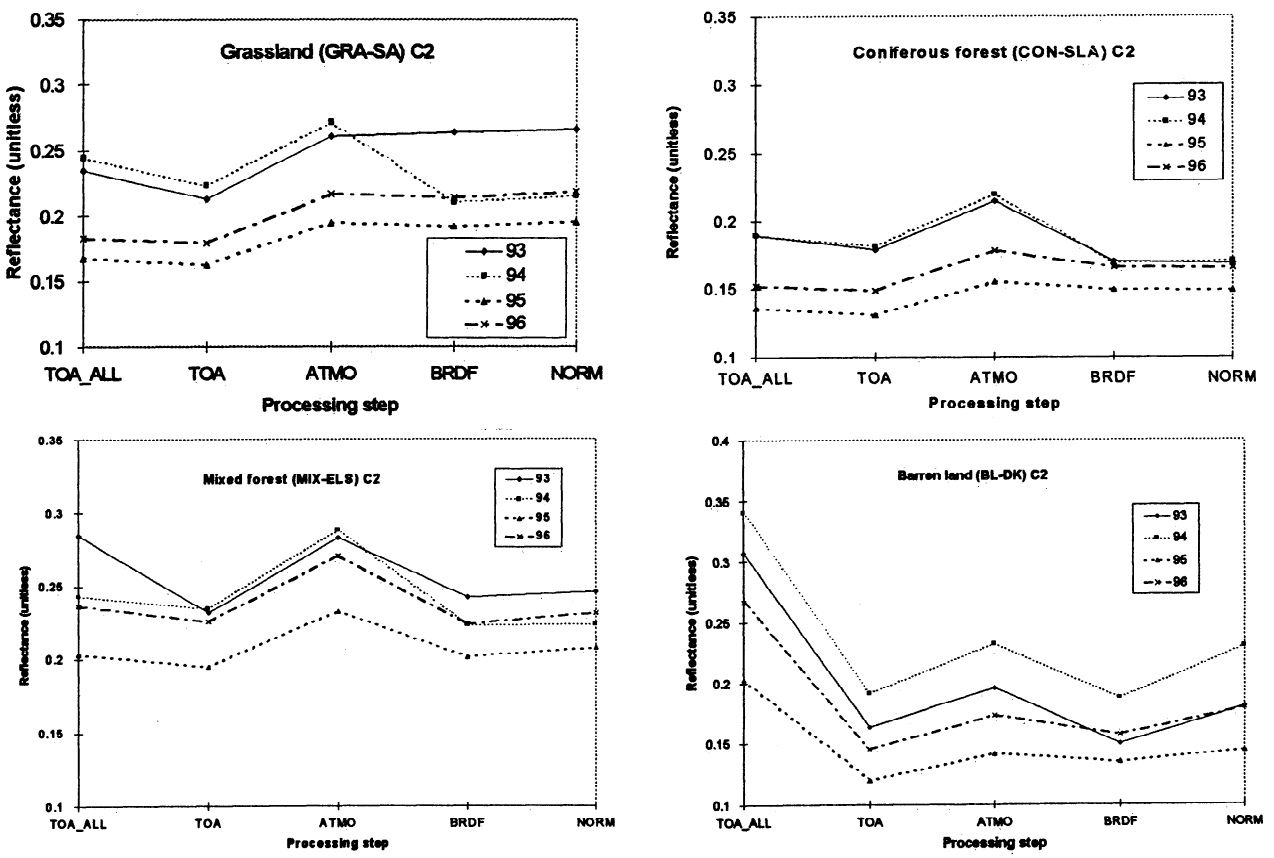

Figure 3. Mean AVHRR channel 2 reflectance for various sites, degree of corrections, and year. TOA, ATMO, BRDF, and NORM refer respectively to data corrected for sensor effects, atmospheric effects, bidirectional effects, and eliminated pixels. The land cover types represented are (a) grassland, (b) coniferous forest, (c) mixed forest, and (d) barren land.

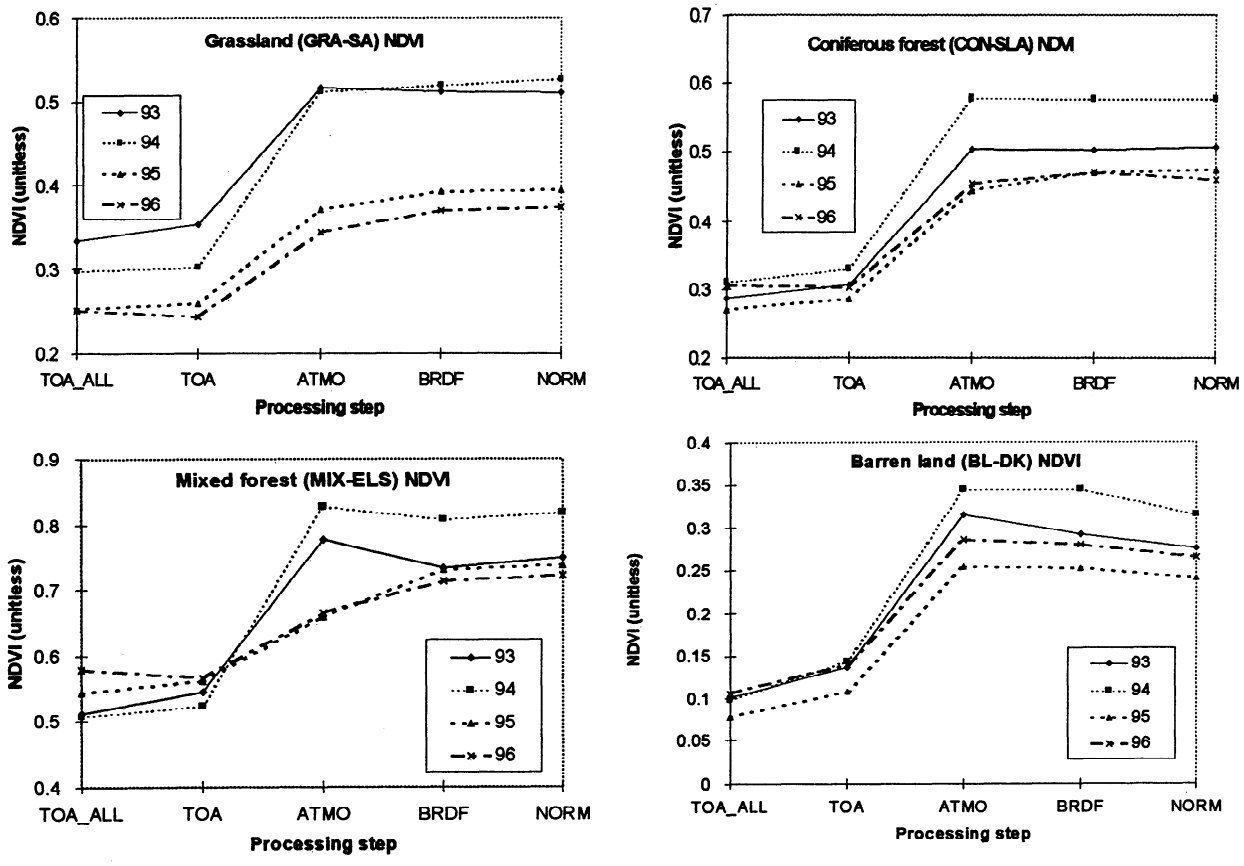

Figure 4. Mean AVHRR NDVI values for various sites, degree of corrections, and year. TOA, ATMO, BRDF, and NORM refer respectively to data corrected for sensor effects, atmospheric effects, bidirectional effects, and eliminated pixels. The land cover types represented are (a) grassland (b) coniferous forest, (c) mixed forest, and (d) barren land.

the NDVI. There was no appreciable difference in the 1994 atmospheric corrections compared to other years. The BRDF corrections had a relatively small effect on the average C2 values for NOAA 14 (1995-1996) but the correction was significant for NOAA 11. This difference was most likely due to the hot spot effect, pronounced over Canada in 1993-1994 and much reduced in 1995 and 1996. Unlike NOAA 11, NOAA 14 AVHRR imaged Canada outside of the principal plane in 1995 and 1996 (about 30°-40°). In this configuration the BRDF effects are significantly reduced, and the hot spot is virtually absent because pronounced hot spot effects are generally found within 30° of the solar angular position [*Chen and Leblanc*, 1997]. As in the case of C1, the BRDF→NORM step had a small effect on the mean values except for barren land.

Figure 4 shows the trends for NDVI means for the same cover types. In all cases the atmospheric corrections sharply increased the NDVI. This follows directly from the respective corrections for C1 and C2 discussed above. The BRDF-related increase was much smaller than that due to atmospheric corrections, as expected from the known dependence of NDVI on cover type and the effects of compositing [*Lee and Kaufman*, 1986; *Cihlar et al.*, 1994; *Wu et al.*, 1995; *Li et al.*, 1996]. Figure 4 also illustrates the land cover dependence of the interannual variability, which was highest for the dynamic vegetation types (e.g., grassland, Figure 4a) and lowest for barren land (Figure 4d). It is worth noting that with the exception of site 1 (grassland), the NDVI in 1994 was higher than in the other years. The range of NDVI values was again smallest for barren land. Given the anomalous behavior of C1 at the BRDF and/or ATMO stages for vegetated cover types (Figures 1a-1c), uncertainties associated with these corrections are probably the dominant factor. As noted above, the relative error in correcting C1 for barren land would be lower because these sites had large SZAs in all four years.

Two other observations should be made regarding Figure 4. One is the consistent difference between the NDVI curves from NOAA 11 (1993, 1994) and NOAA 14, at all processing stages. This is likely related to the differences in the sensing geometry and the ensuing atmospheric and bidirectional corrections. The other is the generally low values for 1995 compared to other years. For all Canada, the mean TOA reflectance was lower by 1% (2.2%) for C1 (C2), lowest values among the four years. This suggests that sensor calibration may also have played an important role in the interannual differences.

4.2. Interannual Variability

If the land surface were the same every year, one would expect to obtain identical mean reflectance values. The variation among years is thus a result of (1) the dynamics of land cover, (2) the measurement and correction errors, or (3) a

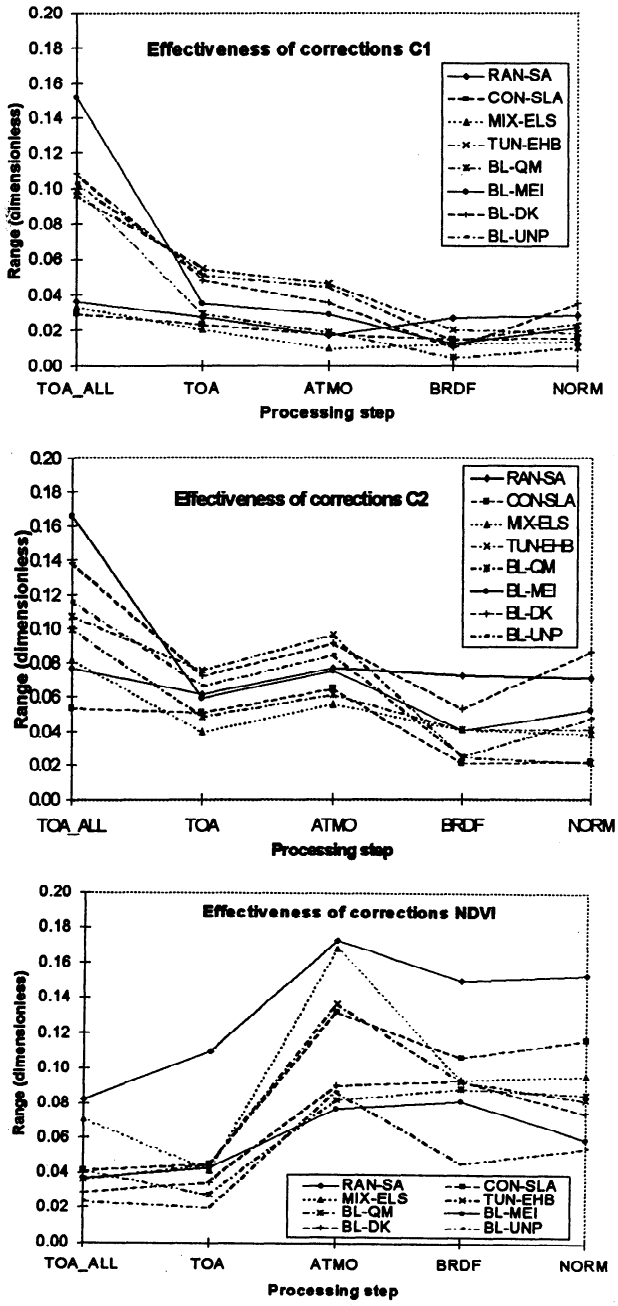

Figure 5. The difference between the maximum and the minimum average values for various sites, degrees of corrections, and years. TOA, ATMO, BRDF, and NORM refer respectively to data corrected for sensor effects, atmospheric effects, bidirectional effects, and eliminated pixels. (a) AVHRR channel 1, (b) AVHRR channel 2, and (c) NDVI are shown. Refer to Table 1 for site description.

combination of the two. For cover types which can be assumed to be mostly time-invariant (e.g., barren land), the interannual variability should therefore indicate the measurement precision.

Figure 5 shows the range of the mean values for a given site and processing stage. For channel 1 (Figure 5a), the range decreased about fourfold between TOA_ALL and the final stage, more for the northern sites. The range decreased monotonically to the BRDF stage at all sites except two. Atmospheric corrections (TOA→ATMO) did not reduce the interannual range appreciably, but BRDF corrections did. The BRDF-related decrease was stronger for barren land than for vegetated cover types. *Chen and Cihlar* [1997] also found larger variations of both AVHRR C1 and C2 reflectance with view angle in barren land than in cropland and forest. The large variations over barren land may be related to shadowing effects of subpixel topography. At the NORM stage, the difference between different cover types was small. The increase betweem BRDF and NORM for some sites is due to imperfect interpolation, caused by too few uncontaminated pixels in northern areas. A similar general trend was observed for channel 2 (Figure 5b). However, atmospheric corrections increased the range (as noted above) and BRDF corrections reduced the range more effectively than for C1. The overall range was reduced about 2.5 times between TOA_ALL and NORM. The NDVI behaved in a more complex way (Figure 5c). The range tended to decrease after removing contaminated pixels (TOA_ALL→TOA), greatly increased after the atmospheric correction as expected, and decreased again once the BRDF corrections were made. The lack of decrease at two sites after BRDF corrections (Figure 5c) is related to the 1994 data (refer to Figure 1). For the other sites, the BRDF correction was more neutral or decreased the observed interannual range. Overall, the interannual range increased between TOA and NORM and provided stronger differentiation between the various cover types.

Considering only the four barren sites (which include sparse vegetation cover or lichen) and weighting the means by the number of pixels at each site, the range of the mean values over the four years was 0.0118 (C1), 0.0418 (C2), and 0.0784 (NDVI) after the BRDF. Since all the sites have some degree of vegetation cover, actual surface interannual changes cannot be completely excluded. Given in addition that the four years represent two different sensors at a fairly extreme viewing geometry, these numbers may be taken as representing a broader range of data acquisition conditions. This is supported by excluding 1994 data when the corresponding values decrease further (0.0110 for C1, 0.0243 for C2, and 0.0381 for NDVI). In either case, these values are the average estimated uncertainty due to the combined sensor calibration, atmospheric corrections, and BRDF correction effects. They do not refer to the uncertainties of individual pixels, which are additionally compromised by random errors in atmospheric and bidirectional corrections as well as by pixel misregistration errors between successive dates.

Since the vegetated sites had higher interannual ranges, these variations must be attributed to the changing surface conditions. For example, the NDVI variation ranged from 0.082 (tundra) to 0.153 (grassland, Figure 5c; 0.082 to 0.136 without 1994), higher than the difference attributable to the measurement uncertainty. This suggests that with the appropriate corrections, AVHRR (and similar data) can be used to detect interannual variations and estimate their magnitude.

4.3. Impact of Measurement Uncertainties on the Detection of Interannual Trends

As an attempt to model the effect of the measurement uncertainties, we examined the impact on the NDVI and the simple ratio SR=C2/C1. Both are commonly used as intermediate variables in deriving biophysical parameters

because of their ability to reduce the correlated noise in these two channels [*Chen*, 1996a]. Figure 6a shows the range between the maximum and the minimum NDVI value per site. The inside points represent the largest difference for that site when only one of the C1 or C2 is measured with an error of 10%; this value is in the range observed at several sites. The inside points were found by computing all combinations of fixed Ci (i=1 or 2) and C≠i, with Ci equal to the mean value per site and C≠i taking on three possible values (mean per site, and +/- 10%). The outside points in Figure 6a show the maximum difference if one assumes that both C1 and C2 are measured with the 10% errors, that is, both Ci and C≠i took on the three possible values. It is seen that the inside points differ by about NDVI=0.1, while the range for the extreme case is about 0.2. Thus the calculations in Figure 6 indicate that NDVI could vary substantially, depending on the uncertainty associated with C1 versus that with C2.

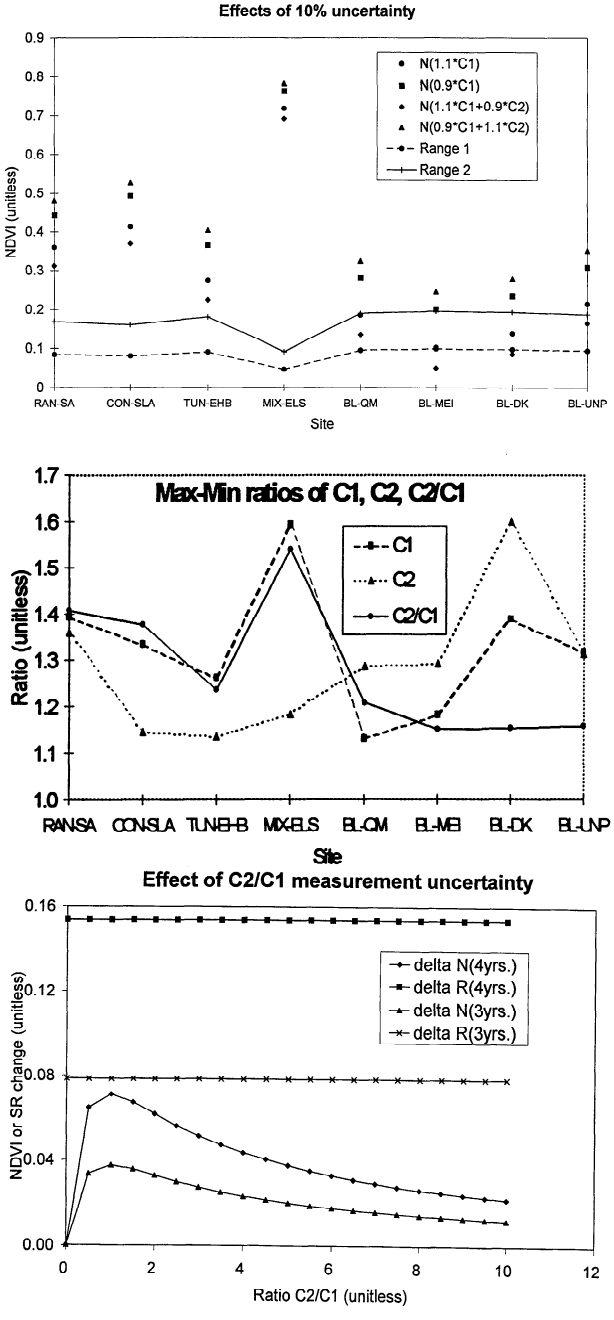

Figure 6. Effects of the AVHRR measurement and correction uncertainties. (a) Effect of 10% difference in AVHRR channel 1 only, channel 2 only, or of both channels.(b) The ratio between the maximum and the minimum average site reflectance during the four years. (c) Effect of the average observed difference in the ratio of AVHRR channel 2 to channel 1 on the NDVI ("delta N") and the simple ratio ("delta R"), for two cases (all four years; and 1993, 1995 and 1996 only).

Among the various uncertainties shown in Figure 6a, which ones are likely? An insight can be obtained from examining the interannual variability of C1, C2, and C2/C1. Figure 6b shows the ratio of highest Ci mean value per site to the lowest Ci over the four years. As observed above, the variations are higher for vegetated sites than for barren land. This is true for both C1 and C2, although the contrast is more pronounced for C1. The simple ratio SR, computed in the same way (the highest SR divided by the lowest SR during the period), behaved in an intermediate manner between the two. Considering the four barren or sparsely vegetated sites, SR varied by about 10%; the weighted mean value was 1.154 (4 years) and 1.078 (without 1994). Generally speaking, if errors in C1 and C2 are uncorrelated, the error in SR would be the sum of these. However, measurement and data processing-induced errors are generally correlated in these two channels, and therefore the error in SR would be smaller than those in the individual channels.

The above values (15.4%, 7.8%) can be taken as representing the uncertainty of SR estimation, because in the case of the other sites, changes in vegetation dynamics may also exhibit strong influence. This is so because radiometric noise effects such as clouds, snow, smoke, and bidirectional variability change both C1 and C2 in the same direction while vegetation changes affect C1 and C2 differently; for example, increase of green vegetation reduces C1 while increasing C2. Using the SR, one can calculate the expected change in NDVI from the above uncertainty (Figure 6c). The NDVI changes by 0.071 or less, depending on the value of the SR. The ΔNDVI values are substantially reduced when taking data from 1993, 1995 and 1996 (Figure 6c). For sites 1-8, SR varied between 1.5 and 7.2. Thus, the errors in NDVI from the measurement uncertainty in C1 and C2 would vary between about 0.029 and 0.068 (all 4 years) or between 0.015 and 0.036 (without 1994). Although small, these are not negligible values. For example, according to a linear relationship between NDVI and leaf area index (LAI) developed by *Chen and Cihlar* [1996], an absolute error of 0.045 in NDVI would cause an absolute error in LAI of 0.9, which is about a 35% relative error for average boreal coniferous forest. The same error in NDVI results in an absolute error of 0.13 in the remotely retrieved fraction of photosynthetically active radiation (FPAR) absorbed by plant canopies based on a linear NDVI-FPAR relationship reported by *Chen* [1996b] for coniferous forests. The equivalent relative error for boreal forests in the summer is 18%. Under nonstressed environmental conditions, the resulting relative error in the estimation of net primary productivity would be about the same as that for FPAR [*Liu et al.*, 1997].

4.4. Discussion

Results presented here show the essential need for post-processing AVHRR composite data for any quantitative use. It is evident that at the TOA level, the data have serious

deficiencies and contain substantial noise. The corrections embedded in the ABC3 procedure are capable of reducing this noise significantly, but their effectiveness depends on the quality of the ancillary information available. Specifically, the atmospheric corrections suffered from the absence of pixel-specific information on the atmospheric composition and very probably also from the degraded performance of the atmospheric correction algorithm at large SZA values. In the case of the BRDF correction, the strategy of deriving the model coefficients separately for each year, originally adopted to obtain higher accuracies, may backfire when the Sun-target-sensor geometry deviates substantially from the nominal case. On balance, a better approach to correcting AVHRR data appears to be the use of fixed coefficients, developed with measurements from several years. Furthermore, the BRDF corrections would benefit from more detailed land cover information since the models could be better tuned to various cover types, and eventually from including topography in BRDF corrections. With this approach, the reduced triplet of errors (0.011 for C1, 0.024 for C2, and 0.038 for NDVI) is achievable even with the current AVHRR data, when averaged over multiple pixels. An important qualifier is that sensor calibration does not introduce an additional uncertainty. This, and the apparent TOA reflectance anomaly in the 1995 data point to the critical importance of accurate sensor calibration. The reasonable interannual consistency confirms the ability of the AVHRR to track surface changes, as also shown by *Goetz* [1997] in a within-season multisensor comparison over grassland.

Since the time series analyzed here covered only four years of data, it is likely that the absolute magnitude of the residual uncertainties would increase over longer periods. On the other hand, the four years included two different AVHRR sensors as well as extreme viewing geometry which introduced additional variability, and the barren sites in most cases contained some vegetation and thus some interannual variability was likely at these sites. In addition, the numbers in Figure 6 represent extreme values observed during this period; the expected values should be substantially smaller. Consequently, the results can be considered characteristic for a broader range of conditions.

5. Summary and Conclusions

Accurate and consistent satellite measurements are essential for monitoring terrestrial vegetation and for assessing interannual trends. Since the remote sensing process inevitably incorporates various types of noise, it is critically important that as many as possible of these errors be removed or isolated. In this study we have evaluated the effectiveness of the ABC3 procedure [*Cihlar et al.*, 1997a] designed to correct AVHRR data over land areas for biospheric studies. Our findings are as follows:

1. Corrections of composite AVHRR data are essential to detect interannual variations. Depending on the measurement of interest (C1, C2, NDVI) and cover type, the most important correction is the removal of contaminated pixels, atmospheric correction, or BRDF correction.

2. The absolute value of C1 and C2 generally decreased between TOA and the normalized surface reflectance with the magnitude of the decrease depending on the AVHRR channel, land cover, and satellite sensor concerned. Conversely, the absolute value of NDVI increased substantially from TOA to surface.

3. The interannual variability in AVHRR C1 and C2 reflectance was reduced substantially after atmospheric and bidirectional corrections, compared to the TOA values. The surface reflectance range was reduced by a factor of approximately 2 to 8, depending on the AVHRR channel and land cover type. The residual variations reflected the remaining noise in the data and the dynamics of vegetation cover. On the other hand, the range of NDVI values increased after the corrections for vegetated cover types, principally due to atmospheric corrections and, second, because of bidirectional reflectance adjustments.

4. Assuming that barren land in northern Canada did not change over the 4 year period, the residual uncertainty in surface reflectance estimation (weighted mean difference for sample areas between the maximum and the minimum over the 4 year period) was 0.012 for C1, 0.042 for C2, and 0.078 for NDVI. Leaving out 1994 data (incomplete bidirectional and atmospheric corrections), the corresponding values are 0.011, 0.024, and 0.038. The latter set appears achievable operationally with AVHRR data, provided sensor calibration does not introduce additional uncertainty. The uncertainties for individual pixels would be higher because of additional random errors in atmospheric, bidirectional, and geometric registration corrections.

5. The impact of the residual uncertainties depends on the way the data are used. When C1 and C2 are used to compute ratios such as the NDVI or the SR, the effect of the uncertainties in the individual bands is reduced substantially because they covary. The weighted mean uncertainty over the 4 years associated with the C2/C1 ratio was 15.4% (7.8% for 3 years) for land with no or sparse vegetation in northern Canada. This results in a 0.028-0.068 (4 years) or 0.015-0.038 (3 years) uncertainty in the NDVI; the latter value is acceptable for land biosphere dynamics studies at northern latitudes.

The above findings lead to three main conclusions. First, corrections of satellite optical measurements for sensor, atmospheric, and bidirectional effects are critical in monitoring interannual trends. Second, procedures such as the ABC3 are effective in removing the noise sources from the multiyear AVHRR data series. Third, improvements in atmospheric corrections (ancillary data and modeling of extreme viewing geometries) are urgently needed for data corrections at northern latitudes. With these improvements, interannual variability of less than 0.015-0.038 in NDVI should be detectable for similar data sets and conditions. An important requirement is that sensor calibration be accurately known. Since any error in the latter will increase these values, the critical importance of accurate sensor calibration cannot be overemphasized.

Acknowledgments. We wish to acknowledge the assistance of Pat Hurlburt from the Manitoba Remote Sensing Centre and Hung Ly from Intermap Technologies with AVHRR data processing. Gunar Fedosejevs from the Canada Centre for Remote Sensing provided constructive comments on a draft of this paper.

References

Ahern, F. J., R.P. Gauthier, P.M. Teillet, J. Sirois, G. Fedosejevs, and D. Lorente, An investigation of continental aerosols with high resolution solar extinction measurements. *Appl. Opt., 30,* 5276-5287, 1991.

Chen, J. M., Evaluation of vegetation indices and a simple ratio for boreal applications, *Can. J. Remote Sens., 22,* 229-242, 1996a.

Chen, J. M., Canopy architecture and remote sensing of the fraction of photosynthetically active radiation in boreal conifer stands, *IEEE Trans. on Geosci. Remote Sens., 34,* 1353-1368, 1996b.

Chen, J. M., and J. Cihlar, Retrieving leaf area index for boreal conifer forests using Landsat TM images, *Remote Sens. Environ., 55,* 153-162, 1996

Chen, J. M., and S. Leblanc, A 4-scale bidirectional reflection model based on canopy architecture, *IEEE Trans. Geosci. Remote Sens, 35,* 1316-1337, 1997.

Chen, J. M., and J. Cihlar, A hot spot function in a simple bidirectional reflectance model for satellite applications, *J. Geophys. Res. 102,* 25, 907-25, 913, 1997.

Cihlar, J., Identification of contaminated pixels in AVHRR composite images for studies of land biosphere, *Remote Sens. Environ. 56,* 149-163, 1996.

Cihlar, J., and F. Huang, Effect of atmospheric correction and viewing angle restriction on AVHRR composites, *Can. J. Remote Sens., 20,* 132-137, 1994.

Cihlar, J., and P.M. Teillet, Forward piecewise linear model for quasi-real time processing of AVHRR data, *Can. J. Remote Sens., 21,* 22-27, 1995.

Cihlar, J., and J. Howarth, Detection and removal of cloud contamination from AVHRR composite images, *IEEE Trans. Geosc. Remote Sens., 32,* 427-437, 1994.

Cihlar, J., D. Manak, and N. Voisin, AVHRR bidirectional reflectance effects and compositing, *Remote Sens. Environ., 48,* 77-88, 1994.

Cihlar, J., H. Ly, Z. Li, J. Chen, H. Pokrant, and F. Huang, Multitemporal, multichannel AVHRR data sets for land biosphere studies - artifacts and corrections, *Remote Sens. Environ., 60,* 35-57, 1997a.

Cihlar, J., J. M. Chen, and Z. Li, Seasonal AVHRR multichannel data sets and products for studies of surface-atmosphere interactions, *J. Geophys. Res., 102,* 29, 625-29, 640, 1997b.

Eidenshink, J.C., and J. L. Faundeen, The 1 km AVHRR global land data set: First stages in implementation, *Int. J. Remote Sens., 15,* 3443-3462, 1994.

European Space Agency, MERIS: The medium resolution imaging spectrometer, *Euro Space Agency Spec. Publ., ESA SP-1184,* 1995.

Goetz, S.J., Multi-sensor analysis of NDVI, surface temperature and biophysical variables at a mixed grassland site, *Int. J. Remote Sens.,* 71-94, 1997.

Gutman, G., Vegetation indices from AVHRR: An update and future prospects, *Remote Sens. Environ., 35,* 121-136, 1991.

Gutman, G., Normalization of multi-annual global AVHRR reflectance data over land surfaces to common Sun-target-sensor geometry, *Adv. Space Res., 14*(1), 121-124, 1994.

Gutman, G., D. Tarpley, A. Igantov, and S. Olson, The enhanced NOAA global land data set from the advanced very high resolution radiometer, *Bull. Am. Meteorol. Soc., 76,* 1141-1156, 1995.

James, M.E., and S.N.V. Kalluri, The Pathfinder AVHRR land data set: An improved coarse resolution data set for terrestrial monitoring, *Int. J. Remote Sens., 15,* 3347-3363, 1994.

Kalnay, E., M. Kanamitsu, R. Kisler, W. Collins, D. Deaven, L. Gandin, M. Iredell, S. Sasha, G. White, J. Woolen, Y. Zhu, M. Chelliah, W. Ebisuzaki, W. Higgins, J. Janowiak, K.C. Mo, C. Ropelewski, J. Wang, A. Leetmaa, R. Reynolds, R. Jenne, and D. Joseph, The NCEP/NCAR 40-year reanalysis project, *Bull. Amer. Meteor. Soc., 77,* 437-471, 1996.

Lee, T.Y., and Y.J. Kaufman, Non-Lambertian effects on remote sensing of surface reflectance and vegetation index, *IEEE Trans. Geosci. Remote Sens., GE-24,* 699-708, 1986.

Li, Z., J. Cihlar, X. Zhang, L. Moreau, and H. Ly, The bidirectional effects of AVHRR measurements over boreal regions, *IEEE Trans. Geosci. Remote Sens. 34,* 1308-1322, 1996.

Liu, J., J. M. Chen, J. Cihlar, and W. Park, A process-based boreal ecosystems productivity simulator using remote sensing inputs, *Remote Sens. Environ.62,* 158-175, 1997.

Los, S.O., C.O. Justice, and C.J. Tucker, A global 1° by 1° NDVI data set for climate studies derived from the GIMMS continental NDVI data, *Int. J. Remote Sens., 15,* 3493-3518, 1994.

Myneni, R.B., C.D. Keeling, C.J. Tucker, G. Asrar, and R.R. Nemani, Increased growth in the northern high latitudes due to enhanced spring time warming, *Nature, 386,* 698-702, 1997.

Pokrant, H., Land cover map of Canada derived from AVHRR images, Manit. Remote Sens. Cent., Winnipeg, Canada, 1991.

Rahman, H., and G. Dedieu, SMAC: A simplified method for the atmospheric correction of satellite measurements in the solar spectrum, *Int. J. Remote Sens., 15,* 123-143, 1994.

Rao, C.R.N., and J. M. Chen, Post-launch calibration of the visible and near infrared channels of the advanced very high resolution radiometer on NOAA-7, -9 and -11 spacecraft, *NOAA Tech. Rep. NESDIS 78,* 22 pp., U.S. Dep. of Commerce, Washington, D.C., 1994.

Rao, C.R.N., J. M. Chen, C.C. Walton, J. T. Sullivan, and M.P. Weinreb, The NOAA/NASA advanced very high resolution radiometer (AVHRR) Pathfinder calibration activity: A progress report, paper presented at Eighth Conference of Atmospheric Radiation, Nashville, Tenn., 1994.

Robertson, B., A. Erickson, J. Friedel, B. Guindon, T. Fisher, R. Brown, P. Teillet, M. D'Iorio, J. Cihlar, and A. Sancz, GEOCOMP, a NOAA AVHRR geocoding and compositing system, paper presented at the International Society of Photogrametry and Remote Sensing Conference, Commission *2,* Washington, D.C., 1992.

Roujean, J.-L., M. Leroy, and P.-Y. Deschamps, A bidirectional reflectance model of the Earth's surface for the correction of remote sensing data, *J. Geophys. Res., 97,*20,455-20,468, 1992.

Saint, G., "VEGETATION" onboard SPOT 4: Mission specifications, *Rep. LERTS 92102,* 40 pp., Lab. d'Etudes et de Rech. en Telédétection Spatiale, Toulouse, France, 1992.

Salomonson, V. V., The moderate resolution imaging spectrometer (MODIS), *IEEE Geosci. Remote Sens. Newslett.,* 11-15, *August,* 1988.

Sellers, P.J., S.O. Los, C.J. Tucker, C.O. Justice, D.A. Dazlich, J.A. Collatz, and D.A. Randall, A global 1° by 1° NDVI data set for climate studies, 2, The generation of global fields of terrestrial biophysical parameters from the NDVI, *Int. J. Remote Sens., 15,* 3519-3545, 1994.

Teillet, P. M., An algorithm for the radiometric and atmospheric correction of AVHRR data in the solar reflective channels, *Remote Sens. Environ., 41,* 185-195, 1992.

Teillet, P.M., and B.N. Holben, Towards operational radiometric calibration of NOAA AVHRR imagery in the visible and near-infrared channels, *Can. J. Remote Sens., 20,* 1-10, 1994.

Townshend, J.R., Global data sets for land applications from the advanced very high resolution radiometer: An introduction. *Int. J. Remote Sens., 15,* 3319-3332, 1994.

Vermote, E., and Y.J. Kaufman, Absolute calibration of AVHRR visible and near-infrared channels using ocean and cloud views, *Int. J. Remote Sens., 16,* 2317-2340, 1995.

Wu, A., Z. Li, and J. Cihlar, Effects of land cover type and greenness on AVHRR bidirectional reflectances: Analysis and removal, *J. Geophys.l Res., 100,* 9179-9192, 1995.

J.M. Chen, J. Cihlar, and Z. Li, Applications Division, Canada Centre for Remote Sensing, 588 Booth Street, Ottawa, ON., Canada, K1A 0Y7. (e-mail: josef.cihlar@ccrs.nrcan.gc.ca)

R. Dixon, Manitoba Remote Sensing Centre, Winnipeg, MB., Canada, R3H 0W4.

F. Huang and R. Latifovic, Intermap Technologies, 2-200 Gurdwara Rd., Nepean, ON., Canada, K2E 1A2.

(Received May 27, 1997; revised November 11, 1997; accepted December 23, 1997.)